

Review

A Review of the Metallogenic Mechanisms of Sandstone-Type Uranium Deposits in Hydrocarbon-Bearing Basins in China

Guihe Li ^{1,2}, Jia Yao ^{2,*} , Yiming Song ³, Jieyun Tang ³, Hongdou Han ³ and Xiangdong Cui ³

¹ School of Engineering and Applied Science, University of Pennsylvania, Philadelphia, PA 19104, USA; guihe@seas.upenn.edu

² College of Engineering and Physical Sciences, University of Wyoming, Laramie, WY 82071, USA

³ Research Institute of Exploration and Development, Liaohe Oilfield Company, CNPC, Panjin 124010, China; songyiming@petrochina.com.cn (Y.S.); tangjy1@petrochina.com.cn (J.T.); hanhd@petrochina.com.cn (H.H.); cuixd@petrochina.com.cn (X.C.)

* Correspondence: jyaouwo@gmail.com

Abstract: As a valuable mineral resource, uranium is extensively utilized in nuclear power generation, radiation therapy, isotope labeling, and tracing. In order to achieve energy structure diversification, reduce dependence on traditional fossil fuels, and promote the sustainable development of energy production and consumption, research on the metallogenic mechanisms and related development technologies of uranium resources has been one of the focuses of China's energy development. Sandstone-type uranium deposits make up approximately 43% of all deposits in China, making them the most prevalent form of uranium deposit there. Sandstone-type uranium deposits and hydrocarbon resources frequently coexist in the same basin in China. Therefore, this study summarizes the spatial and chronological distribution, as well as the geological characteristics, of typical sandstone-type uranium deposits in China's hydrocarbon-bearing basins. From the perspectives of fluid action, geological structure, and sedimentary environment, the metallogenic mechanisms of sandstone-type uranium deposits in hydrocarbon-bearing basins are explored. According to the research, the rapid reduction effect of oil and gas in the same basin is a major factor in the generation of relatively large uranium deposits. Additionally, ions such as CO_3^{2-} and HCO_3^- in hydrothermal fluids of hydrocarbon-bearing basins, which typically originate from dispersed oil and gas, are more conducive to uranium enrichment and sedimentation. This study provides guidance for efficient sandstone-type uranium deposit exploration and production in hydrocarbon-bearing basins and helps to achieve significant improvements in uranium resource exploitation efficiency.

Keywords: hydrocarbon-bearing basins; sandstone-type uranium deposits; metallogenic mechanisms; hydrothermal fluids



Citation: Li, G.; Yao, J.; Song, Y.; Tang, J.; Han, H.; Cui, X. A Review of the Metallogenic Mechanisms of Sandstone-Type Uranium Deposits in Hydrocarbon-Bearing Basins in China. *Eng* **2023**, *4*, 1723–1741. <https://doi.org/10.3390/eng4020098>

Academic Editors: Reza Rezaee and Yujie Yuan

Received: 28 April 2023

Revised: 13 June 2023

Accepted: 15 June 2023

Published: 19 June 2023



Copyright: © 2023 by the authors. Licensee MDPI, Basel, Switzerland. This article is an open access article distributed under the terms and conditions of the Creative Commons Attribution (CC BY) license (<https://creativecommons.org/licenses/by/4.0/>).

1. Introduction

Uranium is a rare mineral resource that is extensively distributed throughout the Earth's crust [1,2], but it typically exists at low concentrations, with an average abundance of about 2.7 ppm (parts per million) [3]. In addition, only a relatively small number of economically viable uranium deposits exist, and they are unevenly distributed [4,5]. Currently, global uranium production is about 54,224 tons [6] and is primarily from countries such as Kazakhstan (43%), Canada (15%), Namibia (11%), and Australia (8%) [7]. Uranium is an important unconventional energy resource primarily used for nuclear power generation [8–10]. Through uranium fission reactions in a nuclear reactor, enormous energy can be generated for electricity production. Nuclear power generation has the advantages of high efficiency and cleanliness [11,12], so it is particularly suitable for areas with high electricity demand, helping to reduce dependence on traditional fossil fuels, and thus reducing carbon emissions [13,14]. In addition, uranium also has other nuclear technology applications, such as radiation therapy [15,16] and isotope labeling and tracing [17,18]. The Organization

for Economic Co-operation and Development (OECD) has provided information that the growing demand for clean energy transition in the future is anticipated to affect nuclear energy capacity, with the East Asia region expected to experience the largest increase in uranium demand [19,20]. To promote the growth of nuclear energy capacity and drive the increase in demand for uranium, it is crucial to acknowledge the benefits of nuclear energy in providing a secure, reliable, and predictable energy supply. Additionally, offering incentives to promote the diversification of low-carbon technologies can help to achieve these goals.

For countries with large populations and rapid economic development, such as China, ensuring energy security is crucial for sustainable development. In order to lower greenhouse gas emissions and combat climate change, the Chinese government has implemented a series of policies [21] to support the development of uranium resources, fully exploiting and utilizing domestic uranium resources to achieve energy diversification, reduce reliance on traditional fossil fuels, and promote sustainable energy production and consumption [22]. China previously aimed to adhere to a strategy referred to as the 'three-third rule' for its uranium supply, which involved one-third coming from domestic mining, one-third from direct international trades, and one-third from Chinese companies mining abroad. However, China's current approach has shifted towards a portfolio approach, where uranium is sourced from various locations based on feasibility and economic viability. The objective is to maximize uranium supply security by utilizing different sources, including those outlined in the 'three-third rule' [23]. Therefore, in recent years, China's uranium mining has also increased, with annual production reaching 1885 tons in 2018, contributing to roughly 4% of global uranium production and ranking among the top ten producers worldwide [24].

Sandstone-type uranium deposits, which are distinguished by their economical in-situ leaching, vast scale, and minimal environmental impact during mining, have become a key area of focus in China's ongoing exploration of uranium resources [25]. Consequently, research into the genesis, exploration, and mining of these deposits has gained significant traction in recent years. The presence of sandstone-type uranium deposits alongside oil and gas resources frequently occurs in China's basins [26–29], indicating a close relationship and coexistence between these resources. This can be attributed to the fact that sandstone, particularly high-porosity and permeability sandstone, functions as a storage space for oil and gas, as well as channels and storage sites for the transportation and enrichment of fluids carrying uranium [30–32]. In addition, the geological structures and sedimentary environments required by hydrocarbon generation and uranium mineralization share certain similarities [33]. The coexistence of hydrocarbon resources and sandstone-type uranium deposits within the same basin offers China a significant advantage in the efficient and economical exploitation of its energy resources. Developed oil and gas basins have relatively complete infrastructure and geological history data that can be directly utilized for uranium exploration and evaluation, leading to comprehensive resource utilization and a substantial improvement in economic efficiency.

However, it should be noted that the metallogenic mechanisms of sandstone-type uranium deposits within hydrocarbon-bearing basins may prove complex because of the presence of varying fluid compositions, geological structures, and sedimentary environments. These factors can have an impact on the enrichment and distribution of uranium. Given the unique features of basins containing both hydrocarbons and sandstone-type uranium deposits, it is imperative to conduct a comprehensive analysis of uranium mineralization in such basins. Therefore, this study presents a comprehensive overview of the geological properties, geographic distribution, and chronological variation of typical sandstone-type uranium deposits found in China's hydrocarbon-bearing basins. By integrating analyses of fluid action, geological structure, sedimentary environment, and other relevant factors, this study elucidates the metallogenic mechanisms underlying sandstone-type uranium deposits within China's hydrocarbon-bearing basins. Findings from this study can enable more precise assessments of uranium reserves, as well as shed light on

the distribution patterns and factors underlying the formation of uranium deposits. The insights gained can inform the exploration and development strategies for sandstone-type uranium deposits, optimizing mining methods and beneficiation processes, and leading to improved efficiency and recovery rates.

2. Characteristics of Sandstone-Type Uranium Deposits in Hydrocarbon-Bearing Basins in China

Figure 1 illustrates the typical forms and distribution percentages of China’s uranium resources, along with their respective locations. The four primary categories of uranium deposits [34] in China are depicted in the figure as follows: sandstone-type, accounting for 43.0% and widely distributed; granite-type, accounting for 22.9% and concentrated in southern China; volcanic-type, accounting for 17.6% and concentrated in eastern China; and C-Si-pelitic type, accounting for 8.7% and concentrated in central and southern China. These four primary categories together contribute to approximately 92.2% of the total confirmed uranium resources in the country [35]. Other types, including alkaline rock type, coal rock type, shale type, and phosphorite type, represent about 7.8% of the total [35]. The geological history of China reveals uranium mineralization events spanning the Palaeoarchean, Early Paleozoic, Late Paleozoic, Triassic, Jurassic, Cretaceous, and Cenozoic eras, as depicted in Figure 2. The Cretaceous and Cenozoic eras were the main period of uranium mineralization [36]. The distribution of these mineralization ages was primarily influenced by China’s tectonic environment [37,38], geological structural evolution [38], and the geochemical properties of uranium elements [39]. The formation of various mountain structures, fault zones, volcanic belts, and sedimentary basins in China, under the influence of tectonic movements, magmatic activity, and sedimentation, has provided suitable environments and conditions for uranium mineralization.

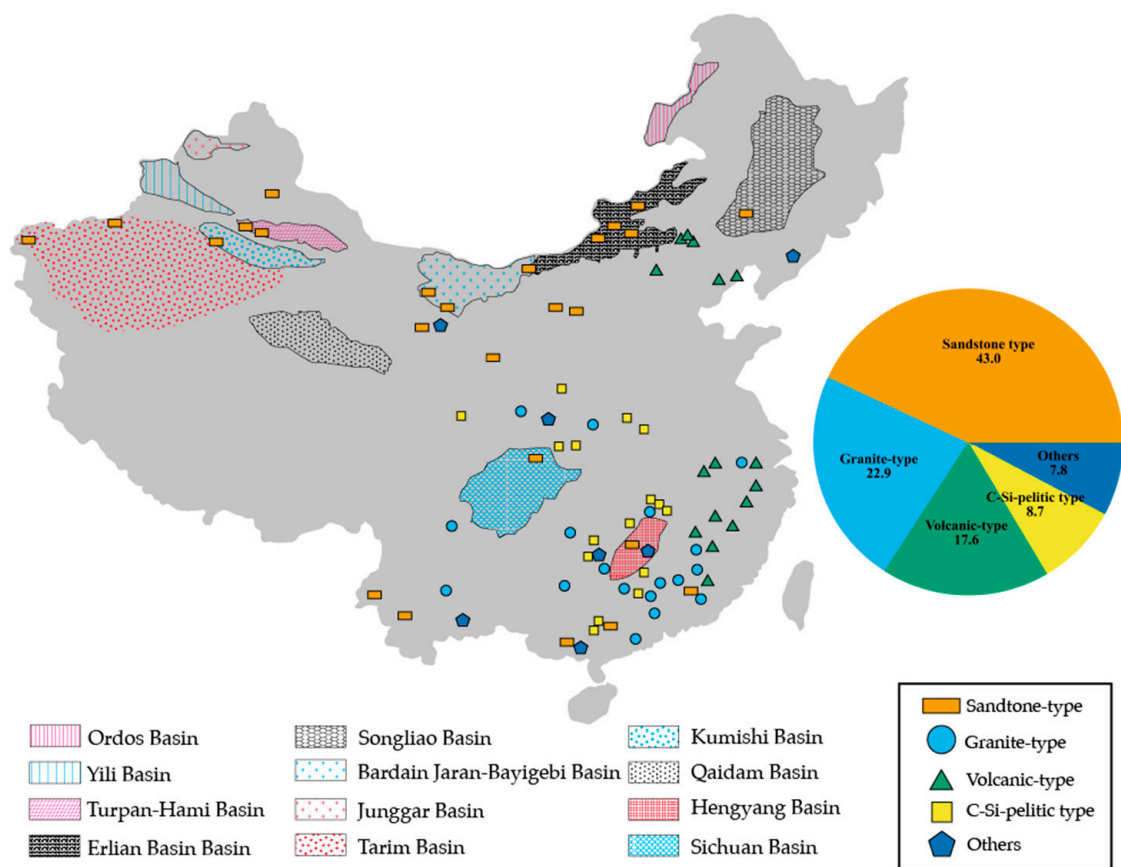


Figure 1. Typical types and distribution percentages and locations of uranium resources in China [40].

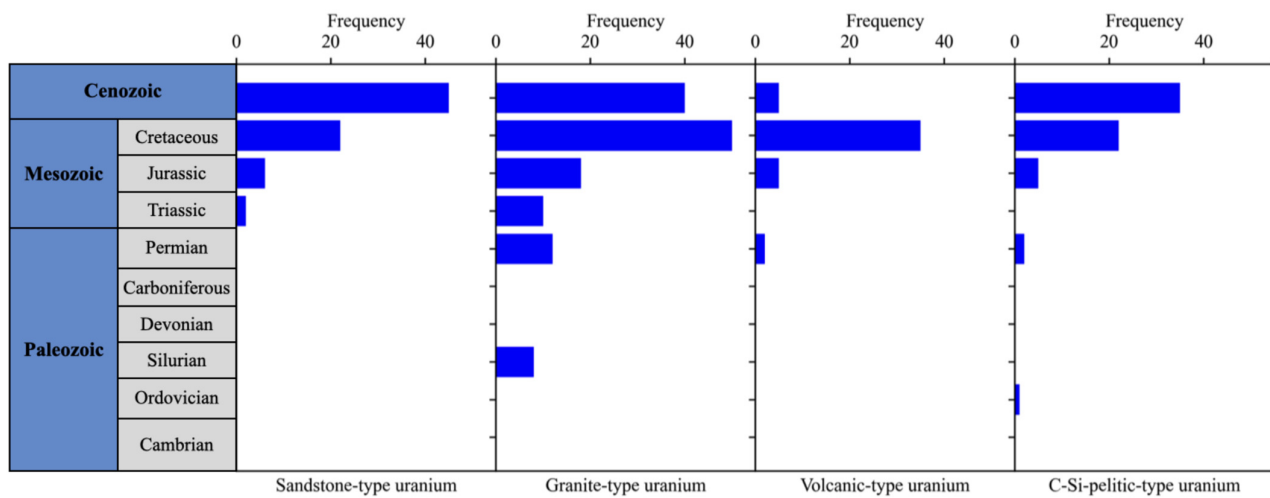


Figure 2. Statistical graph of ore-forming ages of four typical uranium resources in China [35].

Sandstone-type deposits, which make up the majority of China’s confirmed uranium reserves, exhibit certain characteristics in terms of their overall spatial and temporal distribution. Firstly, they are characterized as “small but numerous”. Although individual deposits are small, they are numerous, and have various mineralization geological ages, mineralization periods, and distribution areas [35]. Secondly, they are considered “lean but usable”. Despite China’s uranium resources being mainly of medium to low grades, the ore types are generally good, and the hydrometallurgical processing performance is favorable, making them technically and economically viable [35]. Lastly, they are “widely scattered but relatively concentrated”. Although individual deposits have small scales, they are primarily concentrated in several mining areas and mineralized concentration areas [35].

2.1. Spatial Distribution Characteristics of Sandstone-Type Uranium Deposits in Hydrocarbon-Bearing Basins

Sandstone-type uranium deposits within hydrocarbon-bearing basins are primarily concentrated in China’s large- and medium-sized basins, particularly in the northern region. Among them, six basins, including the Ordos Basin, Yili Basin, Turpan-Hami Basin, Erlian Basin, Songliao Basin, and Badain Jaran-Bayingebi Basin, are projected to hold 75% of China’s entire sandstone-type uranium deposit resources [35]. All these basins are characterized by oil and gas production, with sandstone-type reservoirs being predominant, as well as some shale, mudstone, carbonate hydrocarbon reservoirs, and coalbed methane reservoirs. Table 1 presents the location distribution of the major hydrocarbon-bearing basins in China that are abundant in sandstone-type uranium deposits, along with the burial depth of the hydrocarbon reservoirs and sandstone-type uranium deposits.

Table 1. Distribution of major hydrocarbon-bearing basins and burial depth of their internal hydrocarbon reservoirs and sandstone-type uranium deposits [7,37,41–64].

Hydrocarbon-Bearing Basin	Basin Location	Burial Depth of Hydrocarbon Reservoirs (m)	Burial Depth of Sandstone-Type Uranium Deposits (m)	Resources (tU)
Ordos Basin	In northern China, covering parts of Shaanxi, Inner Mongolia, and Ningxia provinces	2000–4000	300–1500	80,100

Table 1. Cont.

Hydrocarbon-Bearing Basin	Basin Location	Burial Depth of Hydrocarbon Reservoirs (m)	Burial Depth of Sandstone-Type Uranium Deposits (m)	Resources (tU)
Yili Basin	In northern section of Xinjiang Uygur Autonomous Region	1000–4000	200–800	42,700
Turpan-Hami Basin	In northwest section of Xinjiang Uygur Autonomous Region	3000–6000	100–800	10,100
Erlian Basin	In Inner Mongolia	1500–3500	500–1000	52,100
Songliao Basin	In northeastern China, spanning across parts of Liaoning, Jilin, and Heilongjiang provinces	2000–4000	500–1000	16,500
Badain Jaran-Bayingebi Basin	In northwestern China, spanning the provinces of Gansu, Ningxia, and Inner Mongolia	2000–5000	500–1000	7500
Junggar Basin	In northwestern China, covering parts of Xinjiang and Inner Mongolia	2500–15,000	150–1300	N/A
Tarim Basin	In Xinjiang Uygur Autonomous Region	3000–8000	500–3000	N/A
Kumishi Basin	In Xinjiang Uygur Autonomous Region	2000–5000	1000–2000	N/A
Qaidam Basin	In northwestern part of Qinghai province	3000–5000	<3000	N/A
Hengyang Basin	In Hunan province	1500–3000	<1000	N/A
Sichuan Basin	In southwestern China, covering parts of Sichuan, Chongqing, and Guizhou provinces	2000–7000	500–1000	5100

2.2. Temporal Distribution Characteristics of Sandstone-Type Uranium Deposits in Hydrocarbon-Bearing Basins

In China's hydrocarbon-bearing basins, uranium mineralization in sandstone-type deposits spans an extensive temporal range, from the early Mesozoic to the late Cenozoic periods [65]. Figure 2 indicates that the peak periods of uranium mineralization were during the Cretaceous and Cenozoic periods. Table 2 provides information on the formation periods of major hydrocarbon-bearing basins in China, as well as their internal hydrocarbon-bearing reservoirs and sandstone-type uranium deposits. According to Table 2, uranium mineralization primarily occurred in the western basins during the Neogene period, while in the central and eastern basins, it mainly occurred during the Cretaceous period [35].

Table 2. Formation periods of major hydrocarbon-bearing basins, as well as their internal hydrocarbon-bearing reservoirs and sandstone-type uranium deposits [34,42,48,59,66–87].

Hydrocarbon-Bearing Basin	Formation Period of Basin	Main Formation Period of Hydrocarbon-Bearing Layers	Main Mineralization Period of Sandstone-Type Uranium Deposits
Ordos Basin	Paleozoic to Cenozoic	Silurian to Triassic	Jurassic to early Cretaceous
Yili Basin	Late Paleozoic to early Mesozoic	Devonian to Triassic	Triassic to Jurassic
Turpan-Hami Basin	Late Paleozoic to Cenozoic	Permian to early Triassic	Cretaceous

Table 2. *Cont.*

Hydrocarbon-Bearing Basin	Formation Period of Basin	Main Formation Period of Hydrocarbon-Bearing Layers	Main Mineralization Period of Sandstone-Type Uranium Deposits
Erlian Basin	Mesozoic to Cenozoic	Cretaceous to Paleogene	Late Jurassic to early Cretaceous
Songliao Basin	Paleozoic to early Mesozoic	Carboniferous to Jurassic	Carboniferous to Permian
Badain Jaran-Bayingebi Basin	Cenozoic	Neogene	Early to middle Quaternary
Junggar Basin	Late Paleozoic to Mesozoic-Cenozoic	Cretaceous to Neogene	Cretaceous
Tarim Basin	Early Paleozoic to early Cenozoic	Jurassic and Cretaceous	Jurassic to Paleogene
Kumishi Basin	Cenozoic	Neogene	Neogene
Qaidam Basin	Mesozoic to Cenozoic	Neogene	Neogene to Quaternary
Hengyang Basin	Paleozoic	Devonian to Permian	Neogene
Sichuan Basin	Mesozoic to Cenozoic	Cretaceous to Paleogene	Neogene

2.3. Geological Characteristics of Sandstone-Type Uranium Deposits in Hydrocarbon-Bearing Basins

Table 3 summarizes the geological structural characteristics, as well as the sedimentary conditions, of hydrocarbon-bearing basins in China that are rich in sandstone-type uranium resources. Most of these basins have a high prevalence of fault structures, which is a significant factor in their formation and evolution. Some of these basins were formed through marine sedimentation, while others were formed through continental sedimentation that mainly involved lacustrine and fluvial sedimentation. Consequently, the hydrodynamic environment was extremely important during the development process of these basins.

Table 3. Geological structural characteristics and sedimentary conditions of major hydrocarbon-bearing basins [88–108].

Hydrocarbon-Bearing Basin	Geological Structure	Sedimentary Rock	Sedimentary Environment
Ordos Basin	Fault zone and multiple fault structures as primary structural units; Uplifts, and depressions as secondary structural units.	Sandstone, mudstone, coal seam	Continental sedimentation, including coal-bearing strata, ancient lake facies, river facies.
Yili Basin	Fault structures as primary structural units; Reverse faults, slopes, fractures, folds, and uplifts as secondary structural units.	Sandstone and mudstone	Marine sedimentation, including shallow marine facies, continental shelf facies, and marine facies.
Turpan-Hami Basin	Fault zone as primary structural unit; Reverse faults, blind thrust faults, folds, and uplifts as secondary structural units	Sandstone and mudstone	Continental sedimentation, including coal-bearing strata, river facies, and lake facies.
Erlian Basin	Stable structure with only slight structural deformations.	Sandstone, shale, coal seam	Continental sedimentation, including river facies, lake facies, and wind erosion.
Songliao Basin	Fault-rift zone as primary structural unit; Fault blocks, uplifts, depressions, and ancient buried hills as secondary structural units.	Sandstone and mudstone	Marine sedimentation, including shallow marine facies, continental shelf facies, and marine facies.

Table 3. Cont.

Hydrocarbon-Bearing Basin	Geological Structure	Sedimentary Rock	Sedimentary Environment
Badain Jaran-Bayingebi Basin	Fault zone as primary structural unit; Reverse faults, blind thrust faults, slopes, and uplifts as secondary structural units	Sandstone and mudstone	Continental sedimentation, including river facies and lake facies.
Junggar Basin	Fault zone as primary structural unit; Reverse faults, uplifts and depressions as secondary structural units.	Sandstone, mudstone, and carbonate rock	Continental sedimentation, including river facies, lake facies, and wind erosion.
Tarim Basin	Fault zone as primary structural unit; Reverse faults, blind thrust faults, slopes, and uplifts as secondary structural units.	Sandstone and mudstone	Marine sedimentation, including shallow marine facies, continental shelf facies, and marine facies.
Kumishi Basin	Fault zone as primary structural unit; Reverse faults, slopes, and uplifts as secondary structural units.	Sandstone and shale	Continental sedimentation, including river facies, lake facies, and wind erosion.
Qaidam Basin	Fault zone as primary structural unit; Reverse faults, uplifts and depressions as secondary structural units.	Sandstone, mudstone, carbonate rock, and shale.	Marine sedimentation, including shallow marine facies, continental shelf facies, and marine facies.
Hengyang Basin	Fault zone as primary structural unit; Reverse faults, normal faults, and strike-slip faults as secondary structural units.	Sandstone and mudstone	Continental sedimentation, including river facies and lake facies.
Sichuan Basin	Fault zone as primary structural unit; thrust faults, strike-slip faults, normal faults, and uplifts as secondary structural units.	Sandstone, mudstone, shale, and coal seam.	Marine to continental sedimentation.

3. Metallogenic Mechanisms of Sandstone-Type Uranium Deposits in Hydrocarbon-Bearing Basins in China

Sandstone-type uranium deposits are commonly a result of a specific stage in crustal evolution. The main sources of uranium minerals that are present in China's sandstone-type uranium deposits are sedimentary layers within the basin and nearby geological structures that contain significant concentrations of uranium minerals. The redox behavior of uranium ($U^{6+} \rightarrow U^{4+}$) is a fundamental principle followed by uranium mineralization. Uranium minerals are transported and enriched in the form of U^{6+} and ultimately deposited in the sandstone deposits in the form of U^{4+} compounds. Current research among Chinese scholars suggests a consensus regarding the infiltration of fluids in the vicinity of the basin's periphery, which leads to the formation of roll or plate uranium orebodies [109]. Some researchers have proposed that reducing fluids in deep basins are as important during the formation process of these deposits in light of recent advancements in prospecting and research [25]. Moreover, it is suggested that the basin's tectonic movement can cause uranium-bearing fluid to vertically migrate, facilitating uranium deposits to form. Figure 3 illustrates the metallogenic mechanisms involved in the formation process of sandstone-type uranium deposits within basins containing hydrocarbon resources. This study analyzes the mineralization process of sandstone-type uranium within hydrocarbon-bearing basins from the perspective of fluid action to better understand the metallogenic mechanisms involved in sandstone-type uranium deposit formation in such basins. The potential rational theory is clarified in that hydrocarbon-bearing basins are conducive to

sandstone-type uranium mineralization by combining their structural characteristics and sedimentary environment.

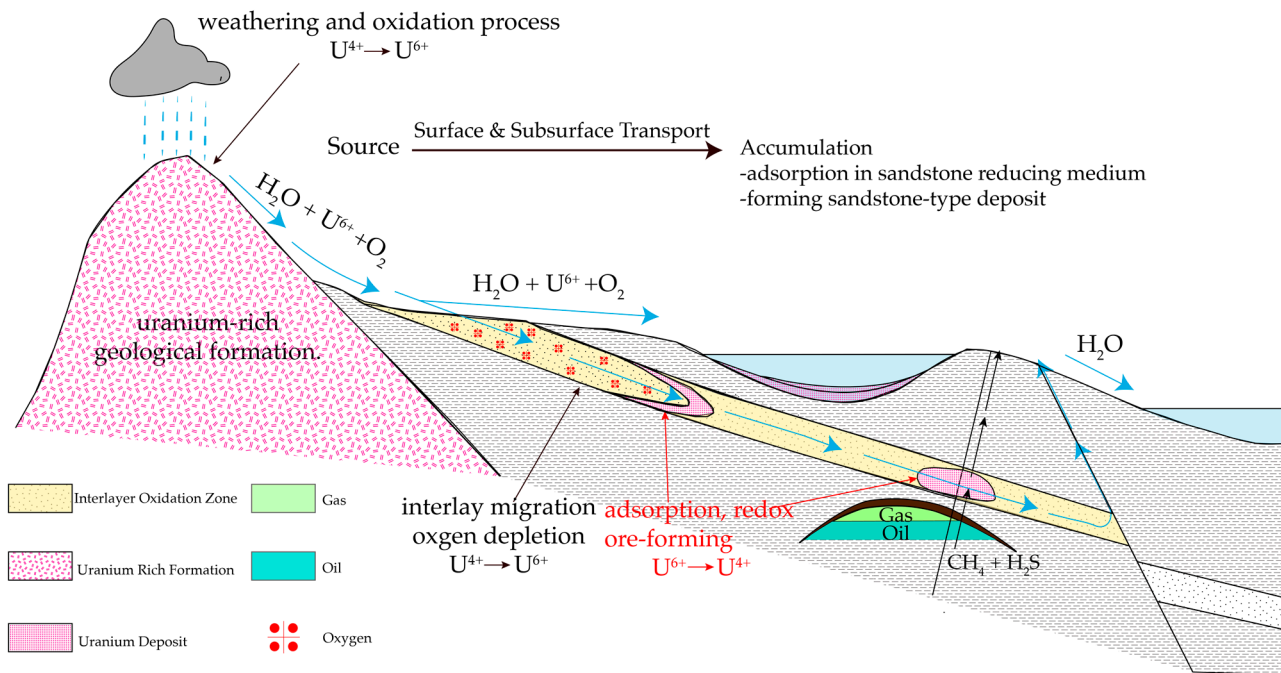


Figure 3. Metallogenic mechanisms of sandstone-type uranium deposits in hydrocarbon-bearing basins [110].

3.1. Fluid Action

The crucial role of fluids in uranium mineralization has been widely recognized in current research. Sandstone-type uranium deposits are formed with the significant involvement of surface water and groundwater. It has been discovered that uranium ore, oil, and gas, as well as low-temperature hydrothermal minerals, can be found in hydrocarbon-bearing basins with extensive sandstone-type uranium resources. This suggests the involvement of low-temperature hydrothermal fluids during uranium mineralization [111,112]. Therefore, this study offers a metallogenic analysis of sandstone-type uranium deposits within hydrocarbon-bearing basins, examining the effects of three fluid types: surface water and groundwater, oil and gas, and hydrothermal fluids.

3.1.1. Action of Surface Water and Groundwater

In uranium-rich hydrocarbon-bearing basins, sandstone-type uranium mineralization primarily occurs through the action of surface water and groundwater, which play a crucial role in providing the hydrodynamic force necessary for uranium mineralization. Under oxidizing conditions, surface water dissolves uranium minerals that are present within the rocks of the surrounding orogenic zone, while groundwater dissolves a significant quantity of uranium-bearing rock debris that is brought into the basin by weathering and denudation. These uranium minerals dissolved by surface water and groundwater can migrate with water flow to the tectonic slope zone, which is favorable for mineralization and enrichment. Under the influence of the siphon effect [113,114] and pulsation cycle mechanism [25], uranium-bearing fluids can promote uranium deposition in sandstone through the form of minerals or adsorptive precipitation. This occurs due to a slowing down of water flow, a decrease in oxygen content in water, and the occurrence of reduction reactions.

3.1.2. Action of Oil and Gas

Uranium deposits and hydrocarbon fields within the same basin are closely intertwined. The spatial location of uranium deposits and the origin of hydrocarbon fields are strongly related. In these hydrocarbon-bearing basins, when sandstones are rich in organic materials, such as fossil plant remains, these organic materials can undergo pyrolysis reactions under the influence of pressure and temperature over an extended length of time, leading to the formation of hydrocarbons. Additionally, these organic materials can also react with uranium-bearing oxidized groundwater as a reducing agent to form uranium deposits. This is because fossil plant remains are abundant in organic matter, including soluble organic matter, fixed organic matter, and structural organic matter, with the majority of it being humus. The organic matter can react with uranium-bearing oxidized groundwater either directly through reduction with bacterial as a catalyst [115], or indirectly through the production of biogenic hydrogen sulfide [116], a reducing agent that causes uranium to precipitate for the deposit formation. Therefore, sandstones that are rich in organic materials within hydrocarbon-bearing basins often become important sites for hydrocarbon generation and uranium deposit mineralization.

However, regarding production stratigraphy and mineralization location, sandstone-type uranium deposits are substantially distinct from hydrocarbon resources. Studies have shown that oil and gas reservoirs are typically located at lower or deeper sections of the sandstone-type uranium-bearing layer within the same basin [117]. In contrast, sandstone-type uranium is primarily mineralized at the top of hydrocarbon reservoirs, especially around the edges of hydrocarbon cap rocks [115]. This up-and-down superposition location association between sandstone-type uranium deposits and hydrocarbon is a key factor in the modification effect of hydrocarbons on uranium deposits.

The spatial distribution of uranium deposits above hydrocarbon reservoirs is determined by their source rock locations and formation processes. As shown in Figure 3, hydrocarbons are mainly derived from organic-rich source rocks, usually located underground or within sedimentary basins, while uranium is derived from uranium-rich minerals in surrounding rocks or debris. Hydrocarbon formation results from the accumulation and maturation of organic matter, while sandstone-type uranium deposition involves the uranium dissolution by surface water or groundwater under oxidizing conditions, the movement of uranium-bearing fluid, and the uranium precipitation under reducing conditions. In basins containing both hydrocarbon resources and sandstone-type uranium deposits, hydrocarbons are usually transported through fractures or unconformities to the overlying or shallow sandstone-type uranium-bearing layers and laterally migrate along the intra-stratigraphic sand body toward the decompression zone [117]. When hydrocarbons encounter oxygenated uranium-bearing fluids or uranium ore bodies, post-generation modification occurs [117] for uranium deposition. Therefore, sandstone-type uranium deposits are usually located above hydrocarbon reservoirs. Chemical analysis of rock samples from drill holes [118] and fluid inclusion tests [119,120] have revealed the presence of hydrocarbon gases, including hydrogen sulfide, carbon dioxide, and methane. These results suggest that hydrocarbon gases, with the function of rapid and local reduction, which leak from oil and gas reservoirs can be utilized as an essential favorable factor to promote larger deposits to form [115]. In addition, sandstone-type uranium deposits are more prone to form within areas with poor sealing at the margins of hydrocarbon reservoirs, as these conditions are more conducive to hydrocarbon infiltration.

Hydrocarbons possess various forms of reducing effects on uranium mineralization depending on their different formation timeframes [117]. Figure 4 presents the initial formation periods of these hydrocarbon-bearing basins, together with those of hydrocarbon reservoirs and uranium deposits contained therein. Within a given basin, the hydrocarbon generation and the sandstone-type uranium deposition may vary, with the possibility of occurring before, concurrently with, and after the latter. When oil and gas are generated earlier than uranium mineralization, they infiltrate the sandstone-type uranium-bearing layer to create a large-scale reducing environment. This increases the reducing capacity within

the mineralized layer, favoring the precipitation and enrichment of uranium. When oil and gas are generated almost simultaneously with uranium mineralization, their infiltration not only increases the reducing capacity but also obstructs the upward migration of oxygenated and uranium-bearing fluids. This leads to the development of a uranium mineralization equilibrium interface, which is a favorable condition for enriched uranium deposits with large scales to form. When oil and gas are generated later than uranium mineralization, their infiltration and reducing modification occur outside the already-formed uranium deposit. This reduces the possible oxidation zone surrounding the deposit and protects the formed uranium mineral body. Additionally, carbonate minerals can form both inside and outside the mining area when hydrocarbons reduce uranium-bearing fluids. Therefore, the presence of carbonate minerals can serve as a valuable indicator or clue for exploring sandstone-type uranium resources.

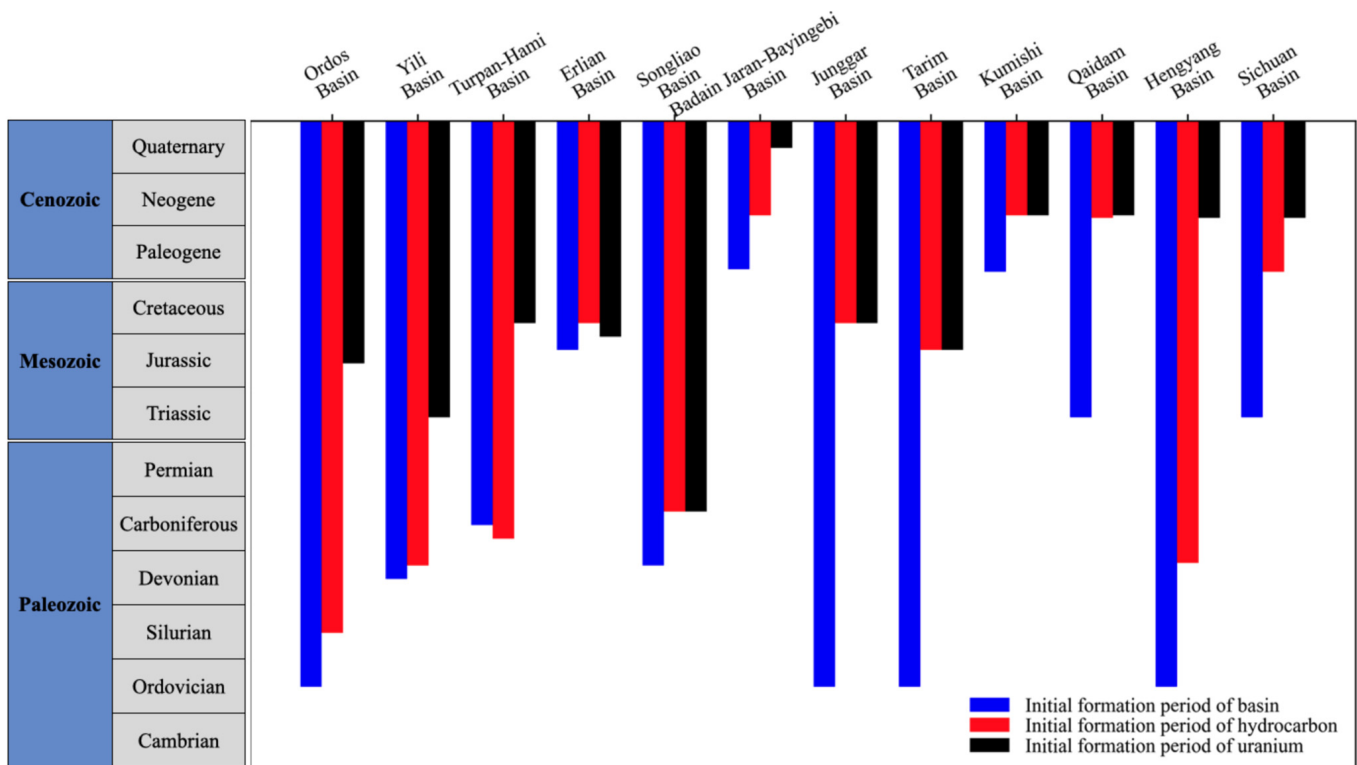


Figure 4. Initial formation periods of hydrocarbon-bearing basins and their internal hydrocarbon reservoirs and sandstone-type uranium deposits.

3.1.3. Action of Hydrothermal Fluids

Hydrothermal fluids form when groundwater at great depths undergoes dissolution of minerals and ions under high temperature and pressure conditions [121]. These fluids are primarily composed of water, dissolved minerals, and ions, which commonly include sodium, potassium, and iron ions.

Hydrothermal fluids found in hydrocarbon-bearing basins not only contain common ions but also CO_3^{2-} and HCO_3^- ions, which are typically sourced from dispersed oil and gas. In a slightly acidic environment, these ions in the hydrothermal fluids can more effectively dissolve U^{6+} . Soluble compounds such as uranyl carbonate complex ions ($[\text{UO}_2(\text{CO}_3)_3]^{4-}$) [122,123] easily form and dissolve in oxygen-containing groundwater, which contributes to the enrichment of uranium ores. These complex anions then react with reducers, such as organic carbon from dispersed oil and gas. As a result, U^{4+} can precipitate under reducing circumstances, which, in turn, further promotes uranium mineralization. Hence, these distinctive compositions of hydrothermal fluids within hydrocarbon-bearing

basins play a pivotal role in the enrichment of uranium during its transportation, thus facilitating the development of larger-scale uranium deposits.

3.2. Geological Structure Effect

Tectonic events in geology refer to the deformation and movement of the Earth's plates, which can cause crustal movements and the formation and evolution of basins. These processes can result in phenomena such as basin uplift, subsidence, and deformation, which significantly affect hydrocarbon generation, transportation, and accumulation, as well as uranium deposition. Table 3 indicates that fault structures are predominant throughout the majority of China's hydrocarbon-bearing basins characterized by abundant sandstone-type uranium resources. This demonstrates that fault movements have a pivotal involvement during the formation process of uranium deposits. Secondary structural units commonly found within these basins are primarily composed of depressions and uplifts.

Faults, as the primary geological structural units, are of vital importance during the developmental and evolutionary processes of hydrocarbon-bearing basins, facilitating both vertical and horizontal migration and the movement of materials. They are able to control the distribution status of sand bodies within these basins and serve as a fundamental area during sandstone-type uranium accumulation [26]. Along with the primary structures, secondary structural units such as depressions and uplifts have the capability to further enhance the abundance of sandstone-type uranium deposits. This is because these units dominate the structural slope zones within the basins, which are the most favorable areas for the accumulation of sand, thereby contributing to the subsequent uranium accumulation for enrichment [124]. Geological processes such as folding and dissolution create favorable storage spaces within the sand bodies, characterized by pores, fractures, and solution cavities, which make it easier for uranium minerals to accumulate. Moreover, basin subsidence causes a significant inflow of groundwater, which promotes the dissolution of uranium in uranium-bearing rocks by groundwater, leading to uranium element enrichment. On the other hand, basin uplift creates a reducing environment for uranium-bearing groundwater, resulting in the conversion of U^{6+} to U^{4+} and precipitation in the form of a compound. Overall, tectonic events and the formation of secondary structures lead to regional differences in movement within the basins, resulting in the large-scale migration and seepage of groundwater and hydrocarbon-related fluids. These processes enhance the effects of groundwater migration and hydrocarbon reduction on uranium mineralization, further promoting the enrichment and mineralization of uranium minerals.

In China, the formation of certain uranium-rich hydrocarbon-bearing basins, such as Tarim Basin, Ordos Basin, and Sichuan Basin, is also influenced by magmatic activities [125]. The uranium-rich geological bodies within the magmatic zones surrounding these basins also significantly contribute to uranium mineralization at vast scales. These geological bodies are primarily composed of uranium-rich granites [126], which provide substantial material for uranium deposition in the uranium-bearing rock series of basins. When these granites intrude into sandstone or other uranium-bearing rocks, the uranium element in the granite is released through chemical reactions [127,128], and then reacts with the surrounding sandstone or other rocks to form uranium minerals. These minerals are further transported and enriched, ultimately forming uranium deposits. Therefore, these uranium-rich granites are crucial uranium sources and are essential catalysts during sandstone-type uranium deposition [129].

3.3. Sedimentary Environment Effect

Figure 4 illustrates that the formation of these hydrocarbon-bearing basins (or their host rocks) generally occurred earlier than their internal uranium mineralization. For non-hydrocarbon-bearing basins, there is no established correlation between basin formation and uranium mineralization. This is due to the fact that the formation time of a basin is determined by its geological background and structure. Typically, crustal movements and tectonic activities such as fault movements, uplift, and subsidence can induce basin

formation. However, hydrocarbon-bearing basins usually have abundant sediment sources and suitable sedimentary environments, in addition to experiencing crustal movements and tectonic activities, which provide sufficient reserve space for the generation and enrichment of hydrocarbons. This abundance of sediment sources and suitable sedimentary environments also create favorable circumstances for uranium deposition. Thus, these factors contribute to the suitability of China's major hydrocarbon-bearing basins for sandstone-type uranium deposition.

Table 1 illustrates that the dominant sedimentary rock types in China's hydrocarbon-bearing basins are sandstone and mudstone. Sandstone serves as the primary medium for the transportation of uranium mineralizing fluids, including uranium-bearing fluids, oil and gas, and hydrothermal fluids. Additionally, it facilitates the accumulation and storage of uranium minerals. The quality of sandstone is governed by its internal heterogeneity and properties, as well as material composition. Sandstones with higher porosity and permeability are better suited for the transport and enrichment of uranium mineralizing fluids. Moreover, the presence of quartz within sandstones promotes a stronger adsorption capacity, thus making quartz-rich sandstones more conducive to the process of uranium mineralization. Mudstone is also a significant accompanying rock [130], and its clay minerals promote uranium deposition through adsorption. Additionally, some hydrocarbon-bearing basins contain carbonate rock, shale, and coal sedimentary rock types. The components of calcite and dolomite in carbonate rocks also employ adsorption [131] to facilitate uranium mineralization, whereas shale and coal seams primarily rely on the reduction effect of their associated organic matter and sulfides to promote uranium enrichment and mineralization.

Furthermore, sandstone-type uranium deposition within hydrocarbon-bearing basins involves hydrodynamics during marine or continental sedimentation. These basins are predominantly situated in system domains with facies characterized by river-dominated deltas and lake margins that are near the source material erosion. The near-source material erosion system [95,132] domains contain plentiful rock debris, organic matter, and other sedimentary materials, which facilitate the formation of thick sedimentary layers and provide ample raw materials, space, and favorable conditions for reduction and adsorption that promote the enrichment and generation of hydrocarbons and uranium. Furthermore, during the sedimentation process, hydrodynamic activities also facilitate the transportation and enrichment of hydrocarbons and uranium to a certain extent.

3.4. Effects of Other Factors

In addition to the primary factors discussed above that influence sandstone-type uranium deposition within hydrocarbon-bearing basins, there are other unique factors that can affect their formation, including paleo-environmental conditions, extreme climates, and biological activity. During the Early to Middle Proterozoic period, the sudden rise in atmospheric oxygen content [133] caused a large amount of previously accumulated uranium in a reduced state to oxidize, dissolve, and migrate, resulting in enrichment and mineralization. In extremely arid climates, strong evaporation can cause uranium to precipitate from sediment pore waters in ancient river valleys, forming uranium deposits [3]. Alternatively, fine sandstones can efficiently adsorb U^{6+} from lake aqueous media to form uranium deposits in environments with strong oxidizing conditions [3]. Low-level animals and plants that are rich in organic matter and propagate in shallow coastal seas can also become uranium deposit hosts and carriers, leading to uranium enrichment [134]. Therefore, these specific mineralization factors must also be considered when analyzing the potential for sandstone-type uranium deposition within hydrocarbon-bearing basins.

4. Conclusions

This study presents a comprehensive analysis and summary of the metallogenic mechanisms and influencing factors associated with sandstone-type uranium deposits within China's hydrocarbon-bearing basins based on their distinct features.

Sandstone-type uranium deposits, which make up the largest proportion of confirmed uranium reserves in China, are mainly distributed in the hydrocarbon-bearing basins in the northern part of the country. The metallogenic mechanisms underlying sandstone-type uranium deposits within these hydrocarbon-bearing basins are mainly influenced by fluid activity, geological structure, and sedimentary environment.

Fluids are of significance during sandstone-type uranium deposition within hydrocarbon-bearing basins. Along with the fundamental mechanism of uranium mineralization through oxidation and reduction by surface water and groundwater, hydrocarbon-bearing basins provide favorable conditions for uranium reduction sedimentation through the availability of organic matter, hydrocarbon gases, and hydrogen sulfide gases. Furthermore, the hydrothermal fluids in these basins can facilitate uranium enrichment and mineralization due to their ability to dissolve CO_3^{2-} and HCO_3^- ions, which are commonly sourced from dispersed oil and gas.

These hydrocarbon-bearing basins commonly have faults as the primary geological structures, and depressions and uplifts as the dominant secondary structures. These geological features provide excellent environments for uranium to accumulate for enrichment. Because of their high porosity and permeability, the sandstones in these basins can facilitate the enrichment and migration of uranium-bearing fluids. The mudstones in these basins promote the sedimentation of uranium ions in fluids through the adsorption capacity of their clay minerals. The formation of these basins involves marine or continental sedimentary processes with the involvement of hydrodynamics, providing sufficient materials, spaces, and favorable reduction and adsorption conditions to enable the enrichment and generation of hydrocarbons and uranium minerals.

The outcomes hold substantial significance in accurately evaluating potential uranium resources, as well as in identifying the distribution patterns and controlling factors of uranium mineral resources. These findings can be employed to guide the exploration and development of sandstone-type uranium resources, thereby enhancing the efficiency of uranium resource utilization.

Author Contributions: All the authors (G.L., J.Y., Y.S., J.T., H.H. and X.C.) have made substantial contributions to this work. G.L.: original draft writing; J.Y.: conceptualization, original draft writing, review and editing; Y.S., J.T., H.H. and X.C.: resources and visualization. All authors have read and agreed to the published version of the manuscript.

Funding: This research is supported by the Prospective Fundamental Technological Research Project of China National Petroleum Corporation, titled "Study on the mineralization mode and enrichment regularity of sandstone-type uranium deposits in hydrocarbon-bearing basins" (2021DJ5301).

Institutional Review Board Statement: Not applicable.

Informed Consent Statement: Not applicable.

Data Availability Statement: Not applicable.

Acknowledgments: The authors are grateful to the Research Institute of Exploration and Development, Liaohe Oilfield Company, CNPC, for the support.

Conflicts of Interest: The authors declare no conflict of interest.

References

1. Charalampides, G.; Vatalis, K.; Karayannis, V.; Baklavaridis, A. Environmental Defects And Economic Impact On Global Market Of Rare Earth Metals. *IOP Conf. Ser. Mater. Sci. Eng.* **2016**, *161*, 012069. [[CrossRef](#)]
2. Herring, J.S. Uranium and Thorium Resources. In *Nuclear Energy*; Springer: New York, NY, USA, 2013; pp. 463–490.
3. Leach, D.L.; Puchlik, K.P.; Glanzman, R.K. Geochemical Exploration for Uranium in Playas. *J. Geochem. Explor.* **1980**, *13*, 251–283. [[CrossRef](#)]
4. Zhang, F.; Jiao, Y.; Wu, L.; Rong, H. Relations between Pyrite Morphologies and Uranium Mineralization in the Shuanglong Region, Northern China. *Ore Geol. Rev.* **2022**, *141*, 104637. [[CrossRef](#)]
5. Zhang, F.; Wang, S.; Jiao, Y.; Wu, L.; Rong, H. Trapping of Uranium by Organic Matter within Sandstones during Mineralization Process: A Case Study from the Shuanglong Uranium Deposit, China. *Ore Geol. Rev.* **2021**, *138*, 104296. [[CrossRef](#)]
6. Peel, R. Nuclear Fuel Reserves. In *Kirk-Othmer Encyclopedia of Chemical Technology*; Wiley: New York, NY, USA, 2021; pp. 1–29.
7. NEA. *Uranium 2022: Resources, Production and Demand*; OECD Publishing: Paris, France, 2023.
8. Hore-Lacy, I. Production of Byproduct Uranium and Uranium from Unconventional Resources. In *Uranium for Nuclear Power*; Elsevier: Amsterdam, The Netherlands, 2016; pp. 239–251.
9. Schaffer, M.B. Abundant Thorium as an Alternative Nuclear Fuel. *Energy Policy* **2013**, *60*, 4–12. [[CrossRef](#)]
10. Pearce, J.M. Limitations of Nuclear Power as a Sustainable Energy Source. *Sustainability* **2012**, *4*, 1173–1187. [[CrossRef](#)]
11. Warner, E.S.; Heath, G.A. Life Cycle Greenhouse Gas Emissions of Nuclear Electricity Generation. *J. Ind. Ecol.* **2012**, *16*, S73–S92. [[CrossRef](#)]
12. Sun, X.; Luo, H.; Dai, S. Ionic Liquids-Based Extraction: A Promising Strategy for the Advanced Nuclear Fuel Cycle. *Chem. Rev.* **2012**, *112*, 2100–2128. [[CrossRef](#)]
13. Brook, B.W.; Alonso, A.; Meneley, D.A.; Misak, J.; Bles, T.; van Erp, J.B. Why Nuclear Energy Is Sustainable and Has to Be Part of the Energy Mix. *Sustain. Mater. Technol.* **2014**, *1–2*, 8–16. [[CrossRef](#)]
14. Ryu, H.; Dorjragchaa, S.; Kim, Y.; Kim, K. Electricity-Generation Mix Considering Energy Security and Carbon Emission Mitigation: Case of Korea and Mongolia. *Energy* **2014**, *64*, 1071–1079. [[CrossRef](#)]
15. Nahar, S.N.; Pradhan, A.K.; Lim, S. K_{α} Transition Probabilities for Platinum and Uranium Ions for Possible X-ray Biomedical Applications. *Can. J. Phys.* **2011**, *89*, 483–494. [[CrossRef](#)]
16. Rump, A.; Eder, S.; Lamkowski, A.; Hermann, C.; Abend, M.; Port, M. A Quantitative Comparison of the Chemo- and Radiotoxicity of Uranium at Different Enrichment Grades. *Toxicol. Lett.* **2019**, *313*, 159–168. [[CrossRef](#)]
17. Malmon, A.G. High Resolution Isotope Tracing in Electron Microscopy Using Induced Nuclear Reactions. *J. Theor. Biol.* **1965**, *9*, 77–92. [[CrossRef](#)] [[PubMed](#)]
18. Brüske, A.; Martin, A.N.; Rammensee, P.; Eroglu, S.; Lazarov, M.; Albut, G.; Schuth, S.; Aulbach, S.; Schoenberg, R.; Beukes, N.; et al. The Onset of Oxidative Weathering Traced by Uranium Isotopes. *Precambrian Res.* **2020**, *338*, 105583. [[CrossRef](#)]
19. Von Hippel, D.F.; Hayes, P. Regional Cooperation for Nuclear Spent Fuel Management in East Asia: Costs, Benefits and Challenges—Part I. *J. Peace Nucl. Disarm.* **2018**, *1*, 305–343. [[CrossRef](#)]
20. Oxford Analytica. *Geopolitical Tensions Cloud Uranium Market*; Oxford Analytica: Oxford, UK, 2022.
21. Yao, J.; Han, H.; Yang, Y.; Song, Y.; Li, G. A Review of Recent Progress of Carbon Capture, Utilization, and Storage (CCUS) in China. *Appl. Sci.* **2023**, *13*, 1169. [[CrossRef](#)]
22. Liu, E.; Lu, X.; Wang, D. A Systematic Review of Carbon Capture, Utilization and Storage: Status, Progress and Challenges. *Energies* **2023**, *16*, 2865. [[CrossRef](#)]
23. Shang, D.; Geissler, B.; Mew, M.; Satalkina, L.; Zenk, L.; Tulsidas, H.; Barker, L.; EI-Yahyaoui, A.; Hussein, A.; Taha, M.; et al. Unconventional Uranium in China's Phosphate Rock: Review and Outlook. *Renew. Sustain. Energy Rev.* **2021**, *140*, 110740. [[CrossRef](#)]
24. Guo, X.; Zhang, X.; Ren, D.; Lin, K. Research on Risk Management and Control Strategy of Uranium Resource Procurement in China. *Energy Sources Part A Recovery Util. Environ. Eff.* **2023**, *45*, 4178–4194. [[CrossRef](#)]
25. Jin, R.; Teng, X.; Li, X.; Si, Q.; Wang, W. Genesis of Sandstone-Type Uranium Deposits along the Northern Margin of the Ordos Basin, China. *Geosci. Front.* **2020**, *11*, 215–227. [[CrossRef](#)]
26. Peng, W.; Liu, Q.; Zhang, Y.; Jia, H.; Zhu, D.; Meng, Q.; Wu, X.; Deng, S.; Ma, Y. The First Extra-Large Helium-Rich Gas Field Identified in a Tight Sandstone of the Dongsheng Gas Field, Ordos Basin, China. *Sci. China Earth Sci.* **2022**, *65*, 874–881. [[CrossRef](#)]
27. Bai, H.; Wang, W.; Lu, Q.; Wang, W.; Feng, S.; Zhang, B. Geological Characteristics and Control Mechanism of Uranium Enrichment in Coal-Bearing Strata in the Yili Basin, Northwest China—Implications for Resource Development and Environmental Protection. *ACS Omega* **2022**, *7*, 5453–5470. [[CrossRef](#)] [[PubMed](#)]
28. Hu, S.; Hu, H.; Shi, E.; Tang, C.; Zhang, R.; Hao, Y. Seismic Interpretation of Sandstone-Type Uranium Deposits in the Songliao Basin, Northeast China. *Interpretation* **2022**, *10*, T665–T679. [[CrossRef](#)]
29. Zhu, Q.; Li, J.; Li, G.; Wen, S.; Yu, R.; Tang, C.; Feng, X.; Liu, X. Characteristics of Sandstone-Type Uranium Mineralization in the Hangjinqi Region of the Northeastern Ordos Basin: Clues from Clay Mineral Studies. *Ore Geol. Rev.* **2022**, *141*, 104642. [[CrossRef](#)]
30. Richards, M.C.; Issen, K.A.; Ingraham, M.D. A Coupled Elastic Constitutive Model for High Porosity Sandstone. *Int. J. Rock Mech. Min. Sci.* **2022**, *150*, 104989. [[CrossRef](#)]

31. Zhang, P.; Yu, C.; Zeng, X.; Tan, S.; Lu, C. Ore-controlling Structures of Sandstone-Hosted Uranium Deposit in the Southwestern Ordos Basin: Revealed from Seismic and Gravity Data. *Ore Geol. Rev.* **2022**, *140*, 104590. [[CrossRef](#)]
32. Ren, Y.; Yang, X.; Hu, X.; Wei, J.; Tang, C. Mineralogical and Geochemical Evidence for Biogenic Uranium Mineralization in Northern Songliao Basin, NE China. *Ore Geol. Rev.* **2022**, *141*, 104556. [[CrossRef](#)]
33. Mukherjee, S.; Goswami, S.; Zakauilla, S. Geological Relationship between Hydrocarbon and Uranium: Review on Two Different Sources of Energy and the Indian Scenario. *Geoenergy Sci. Eng.* **2023**, *221*, 111255. [[CrossRef](#)]
34. Zhang, C.; Cai, Y.-Q.; Dong, Q.; Xu, H. Cretaceous–Neogene Basin Control on the Formation of Uranium Deposits in South China: Evidence from Geology, Mineralization Ages, and H–O Isotopes. *Int. Geol. Rev.* **2020**, *62*, 263–310. [[CrossRef](#)]
35. Cai, Y.; Zhang, J.; Li, Z.; Guo, Q.; Song, J.; Fan, H.; Liu, W.; Qi, F. Outline of Uranium Resources Characteristics and Metallogenetic Regularity in China. *Acta Geol. Sin.* **2015**, *89*, 1051–1069.
36. Hou, B.; Keeling, J.; Li, Z. Paleovalley-Related Uranium Deposits in Australia and China: A Review of Geological and Exploration Models and Methods. *Ore Geol. Rev.* **2017**, *88*, 201–234. [[CrossRef](#)]
37. Cheng, Y.; Wang, S.; Zhang, T.; Teng, X.; Ao, C.; Jin, R.; Li, H. Regional Sandstone-Type Uranium Mineralization Rooted in Oligo–Miocene Tectonic Inversion in the Songliao Basin, NE China. *Gondwana Res.* **2020**, *88*, 88–105. [[CrossRef](#)]
38. Han, X.; Wu, Z.; Ji, H.; Jiang, Z.; Guo, Y.; Lin, Z.; Hu, H.; Yin, D. Constraints of Tectonic Uplift and Denudation on Sandstone-Type Uranium Mineralization in Meso-Cenozoic Basins in Northern China: A Review. *Ore Geol. Rev.* **2021**, *139*, 104528. [[CrossRef](#)]
39. Ren, Y.; Yang, X.; Miao, P.; Hu, X.; Chen, Y.; Chen, L.; Zhao, H. Mineralogical and Geochemical Research on Pengyang Deposit: A Peculiar Eolian Sandstone-Hosted Uranium Deposit in the Southwest of Ordos Basin. *Ore Geol. Rev.* **2022**, *141*, 104571. [[CrossRef](#)]
40. Xu, D.; Chi, G.; Nie, F.; Fayek, M.; Hu, R. Diversity of Uranium Deposits in China—An Introduction to the Special Issue. *Ore Geol. Rev.* **2021**, *129*, 103944. [[CrossRef](#)]
41. Luo, J.L.; Morad, S.; Salem, A.; Ketzer, J.M.; Lei, X.L.; Guo, D.Y.; Hlal, O. Impact of Diagenesis on Reservoir-Quality Evolution in Fluvial and Lacustrine-Deltaic Sandstones: Evidence from Jurassic and Triassic Sandstones from the Ordos Basin, China. *J. Pet. Geol.* **2009**, *32*, 79–102. [[CrossRef](#)]
42. Jiao, Y.; Wu, L.; Rong, H.; Peng, Y.; Miao, A.; Wang, X. The Relationship between Jurassic Coal Measures and Sandstone-Type Uranium Deposits in the Northeastern Ordos Basin, China. *Acta Geol. Sin.-Engl. Ed.* **2016**, *90*, 2117–2132. [[CrossRef](#)]
43. Jin, R.; Yu, R.; Miao, P. *Basin Uranium Mineralization Law*; Springer: Singapore, 2023; pp. 325–356.
44. Liu, Z.Y.; Peng, S.P.; Qin, M.K.; Liu, H.X.; Geng, Y.Y.; Zhang, X.; Ding, B.; Xiu, X.Q. Origin and Role of Kaolinization in Roll-Front Uranium Deposits and Its Response to Ore-Forming Fluids in the Yili Basin, China. *Geofluids* **2018**, *2018*, 7847419. [[CrossRef](#)]
45. Chen, Y.; Li, J.; Wang, X.; Wang, Z.; Wei, Y.; Ren, J. Occurrence Characteristics and Influencing Factors of Uranium and Radon in Deep-Buried Thermal Storage Aquifers. *J. Radioanal. Nucl. Chem.* **2022**, *331*, 755–767. [[CrossRef](#)]
46. Qian, C.; Yang, S.; Wang, Y.; Wu, C.; Zhang, Y. Prediction and Modeling of Petrophysical Parameters of Deep-Buried, Low Permeability Glutenite Reservoirs in Yubei Area, Turpan-Hami Basin, China. *J. Pet. Sci. Eng.* **2021**, *207*, 109154. [[CrossRef](#)]
47. Liu, B.; Shi, Z.; Peng, Y.; Zhang, P.; Li, P. Sequence Stratigraphy of the Lower Cretaceous Uraniferous Measures and Mineralization of the Sandstone-hosted Tamusu Large Uranium Deposit, North China. *Acta Geol. Sin.-Engl. Ed.* **2022**, *96*, 167–192. [[CrossRef](#)]
48. Zuo, Y.; Wang, C.; Tang, S.; Hao, Q. Mesozoic and Cenozoic Thermal History and Source Rock Thermal Evolution of the Baiyinchagan Sag, Erlian Basin, Northern China. *J. Pet. Sci. Eng.* **2016**, *139*, 171–184. [[CrossRef](#)]
49. Wu, Q.; Wang, Y.; Li, Z.; Qiao, B.; Yu, X.; Huang, W.; Cao, C.; Li, Z.; Pan, Z.; Huang, Y. 2D and 3D Seismic Survey for Sandstone-Type Uranium Deposit and Its Prediction Patterns, Erlian Basin, China. *Minerals* **2022**, *12*, 559. [[CrossRef](#)]
50. Xi, K.; Cao, Y.; Jähren, J.; Zhu, R.; Bjørlykke, K.; Haile, B.G.; Zheng, L.; Hellevang, H. Diagenesis and Reservoir Quality of the Lower Cretaceous Quantou Formation Tight Sandstones in the Southern Songliao Basin, China. *Sediment. Geol.* **2015**, *330*, 90–107. [[CrossRef](#)]
51. Yao, J.; Li, G.; Wu, J. Application of In-Situ Combustion for Heavy Oil Production in China: A Review. *J. Oil Gas Petrochem. Sci.* **2018**, *1*, 69–72. [[CrossRef](#)]
52. Yao, J.; Song, Y. Dynamic Analysis Approach to Evaluate In-Situ Combustion Performance for Heavy Oil Production. *J. Oil Gas Petrochem. Sci.* **2019**, *2*, 42–47. [[CrossRef](#)]
53. Cao, B.; Luo, X.; Zhang, L.; Sui, F.; Lin, H.; Lei, Y. Diagenetic Evolution of Deep Sandstones and Multiple-Stage Oil Entrapment: A Case Study from the Lower Jurassic Sangonghe Formation in the Fukang Sag, Central Junggar Basin (NW China). *J. Pet. Sci. Eng.* **2017**, *152*, 136–155. [[CrossRef](#)]
54. Clayton, J.L.; Yang, J.; King, J.D.; Lillis, P.G.; Warden, A. Geochemistry of Oils from the Junggar Basin, Northwest China. *Am. Assoc. Pet. Geol. Bull.* **1997**, *81*, 1926–1944. [[CrossRef](#)]
55. Huang, S.; Qin, M.; Liu, Z.; He, Z.; Geng, Y. Litho-mineralogy, Geochemistry, and Chronology for the Genesis of the Kamust Sandstone-hosted Uranium Deposit, Junggar Basin, NW China. *Geol. J.* **2022**, *57*, 1530–1551. [[CrossRef](#)]
56. Liu, S.; Lei, X.; Feng, C.; Hao, C. Estimation of Subsurface Formation Temperature in the Tarim Basin, Northwest China: Implications for Hydrocarbon Generation and Preservation. *Int. J. Earth Sci.* **2016**, *105*, 1329–1351. [[CrossRef](#)]
57. Cai, C.; Qiu, N.; Soares, C.J.; Chen, H. Study on the Detrital Zircon Fission-track Ages from Natural Borehole Samples in the Bohai Bay and Tarim Basins with Different Thermal Backgrounds. *Geol. J.* **2021**, *56*, 4189–4200. [[CrossRef](#)]

58. Zhu, G.; Li, J.; Zhang, Z.; Wang, M.; Xue, N.; He, T.; Zhao, K. Stability and Cracking Threshold Depth of Crude Oil in 8000 m Ultra-Deep Reservoir in the Tarim Basin. *Fuel* **2020**, *282*, 118777. [[CrossRef](#)]
59. Liu, C.; Huang, L.; Zhao, H.; Wang, J.; Zhang, L.; Deng, Y.; Zhao, J.; Zhang, D.; Fan, C. Small-Scale Petroliferous Basins in China: Characteristics and Hydrocarbon Occurrence. *Am. Assoc. Pet. Geol. Bull.* **2019**, *103*, 2139–2175. [[CrossRef](#)]
60. Huang, C.; Yuan, X.; Song, C.; Yuan, J.; Ni, X.; Ma, X.; Zhang, S. Characteristics, Origin, and Role of Salt Minerals in the Process of Hydrocarbon Accumulation in the Saline Lacustrine Basin of the Yingxi Area, Qaidam, China. *Carbonates Evaporites* **2018**, *33*, 431–446. [[CrossRef](#)]
61. Ma, X.; Huang, C.; Shi, Y. Oil and Gas Enrichment Patterns and Major Controlling Factors for Stable and High Production of Tight Lacustrine Carbonate Rocks, a Case Study of Yingxi Area in Qaidam Basin, West China. *Carbonates Evaporites* **2019**, *34*, 1815–1831. [[CrossRef](#)]
62. He, Z.; Feng, J.; Luo, J.; Zeng, Y. Distribution, Exploitation, and Utilization of Intermediate-to-Deep Geothermal Resources in Eastern China. *Energy Geosci.* **2023**, *4*, 100187. [[CrossRef](#)]
63. Zhou, Q.; Xiao, X.; Tian, H.; Pan, L. Modeling Free Gas Content of the Lower Paleozoic Shales in the Weiyuan Area of the Sichuan Basin, China. *Mar. Pet. Geol.* **2014**, *56*, 87–96. [[CrossRef](#)]
64. Chen, S.; Zhu, Y.; Qin, Y.; Wang, H.; Liu, H.; Fang, J. Reservoir Evaluation of the Lower Silurian Longmaxi Formation Shale Gas in the Southern Sichuan Basin of China. *Mar. Pet. Geol.* **2014**, *57*, 619–630. [[CrossRef](#)]
65. Liu, C.; Qiu, X.; Wu, B.; Zhao, H. Subdivisions of the Central-East Asia Multi-Energy Minerals Metallogenetic Domain and Types of Those Basins. *Energy Explor. Exploit.* **2009**, *27*, 153–166. [[CrossRef](#)]
66. Tang, X.; Zhang, J.; Shan, Y.; Xiong, J. Upper Paleozoic Coal Measures and Unconventional Natural Gas Systems of the Ordos Basin, China. *Geosci. Front.* **2012**, *3*, 863–873. [[CrossRef](#)]
67. Wang, P.; Zhang, C.; Li, X.; Zhang, K.; Yuan, Y.; Zang, X.; Cui, W.; Liu, S.; Jiang, Z. Organic Matter Pores Structure and Evolution in Shales Based on the He Ion Microscopy (HIM): A Case Study from the Triassic Yanchang, Lower Silurian Longmaxi and Lower Cambrian Niutitang Shales in China. *J. Nat. Gas Sci. Eng.* **2020**, *84*, 103682. [[CrossRef](#)]
68. Jolivet, M.; Heilbronn, G.; Robin, C.; Barrier, L.; Bourquin, S.; Guo, Z.; Jia, Y.; Guerit, L.; Yang, W.; Fu, B. Reconstructing the Late Palaeozoic–Mesozoic Topographic Evolution of the Chinese Tian Shan: Available Data and Remaining Uncertainties. *Adv. Geosci.* **2013**, *37*, 7–18. [[CrossRef](#)]
69. Liu, D.; Jolivet, M.; Yang, W.; Zhang, Z.; Cheng, F.; Zhu, B.; Guo, Z. Latest Paleozoic–Early Mesozoic Basin–Range Interactions in South Tian Shan (Northwest China) and Their Tectonic Significance: Constraints from Detrital Zircon U–Pb Ages. *Tectonophysics* **2013**, *599*, 197–213. [[CrossRef](#)]
70. Chen, C.; Lu, H.; Jia, D.; Cai, D.; Wu, S. Closing History of the Southern Tianshan Oceanic Basin, Western China: An Oblique Collisional Orogeny. *Tectonophysics* **1999**, *302*, 23–40. [[CrossRef](#)]
71. Han, B.-F.; He, G.-Q.; Wang, X.-C.; Guo, Z.-J. Late Carboniferous Collision between the Tarim and Kazakhstan–Yili Terranes in the Western Segment of the South Tian Shan Orogen, Central Asia, and Implications for the Northern Xinjiang, Western China. *Earth Sci. Rev.* **2011**, *109*, 74–93. [[CrossRef](#)]
72. Novikov, I.S. Reconstructing the Stages of Orogeny around the Junggar Basin from the Lithostratigraphy of Late Paleozoic, Mesozoic, and Cenozoic Sediments. *Russ. Geol. Geophys.* **2013**, *54*, 138–152. [[CrossRef](#)]
73. Allen, M.B.; Engör, A.M.C.; Natal'in, B.A. Junggar, Turfan and Alakol Basins as Late Permian to? Early Triassic Extensional Structures in a Sinistral Shear Zone in the Altaid Orogenic Collage, Central Asia. *J. Geol. Soc. Lond.* **1995**, *152*, 327–338. [[CrossRef](#)]
74. Xin, Z.; Fengjun, N.; Xuebin, S.; Fei, X.; Mangan, L.; Zhaobin, Y.; Chengyong, Z.; Zhibing, F. Relationships between Meso-Cenozoic Denudation in the Eastern Tian Shan and Uranium Mineralization in the Turpan-Hami Basin, NW China: Constraints from Apatite Fission Track Study. *Ore Geol. Rev.* **2020**, *127*, 103820. [[CrossRef](#)]
75. Zhao, X.; Jin, F.; Wang, Q.; Han, C.; Kang, R. Theory of Hydrocarbon Accumulation in Troughs within Continental Faulted Basins and Its Application: A Case Study in Jizhong Depression and Erlian Basin. *Acta Pet. Sin.* **2011**, *32*, 18–24.
76. Wang, Y.; Zhang, F.; Zhang, D.; Miao, L.; Li, T.; Xie, H.; Meng, Q.; Liu, D. Zircon SHRIMP U–Pb Dating of Meta-Diorite from the Basement of the Songliao Basin and Its Geological Significance. *Chin. Sci. Bull.* **2006**, *51*, 1877–1883. [[CrossRef](#)]
77. Lu, J.; Luo, Z.; Zou, H.; Li, Y.; Hu, Z.; Zhou, Z.; Zhu, J.; Han, M.; Zhao, L.; Lin, Z. Geochemical Characteristics, Origin, and Mechanism of Differential Accumulation of Natural Gas in the Carboniferous Kelameili Gas Field in Junggar Basin, China. *J. Pet. Sci. Eng.* **2021**, *203*, 108658. [[CrossRef](#)]
78. Chen, Y.; Miao, P.; Li, J.; Jin, R.; Zhao, H.; Chen, L.; Wang, C.; Yu, H.; Zhang, X. Association of Sandstone-Type Uranium Mineralization in the Northern China with Tectonic Movements and Hydrocarbons. *J. Earth Sci.* **2022**, *33*, 289–307. [[CrossRef](#)]
79. Allen, M.B.; Vincent, S.J.; Wheeler, P.J. Late Cenozoic Tectonics of the Kepingtage Thrust Zone: Interactions of the Tien Shan and Tarim Basin, Northwest China. *Tectonics* **1999**, *18*, 639–654. [[CrossRef](#)]
80. Sobel, E.R. Basin Analysis of the Jurassic–Lower Cretaceous Southwest Tarim Basin, Northwest China. *Geol. Soc. Am. Bull.* **1999**, *111*, 709–724. [[CrossRef](#)]
81. Shi, P.; Fu, B.; Ma, Y.; Guo, Q.; Xu, H. Remote Sensing Detection for Surface Anomalies Related to Hydrocarbon in Bashibulake Uranium Ore, Southern Tianshan. In Proceedings of the 2016 IEEE International Geoscience and Remote Sensing Symposium (IGARSS), Beijing, China, 10–15 July 2016; IEEE: New York, NY, USA, 2016; pp. 6374–6377.

82. Ren, G.; Li, C.; Wu, C.; Zhang, H.; Wang, S.; Ren, Z.; Lei, Q.; Li, X. Late Quaternary Slip Rate and Kinematics of the Baoertu Fault, Constrained by ¹⁰Be Exposure Ages of Displaced Surfaces within Eastern Tian Shan. *Lithosphere* **2021**, *2021*, 7866920. [[CrossRef](#)]
83. Cheng, F.; Guo, Z.; Jenkins, H.S.; Fu, S.; Cheng, X. Initial Rupture and Displacement on the Altyn Tagh Fault, Northern Tibetan Plateau: Constraints Based on Residual Mesozoic to Cenozoic Strata in the Western Qaidam Basin. *Geosphere* **2015**, *11*, 921–942. [[CrossRef](#)]
84. Sun, P.; Guo, Z.; He, W.; Liu, W. Restoration of Eroded Thickness of the Neogene Strata in the Western Qaidam Basin and Its Significance for Oil and Gas Occurrence. *Acta Geol. Sin.-Engl. Ed.* **2017**, *91*, 1352–1362. [[CrossRef](#)]
85. Abudukeyumu, A.; Song, H.; Chi, G.; Li, Q.; Zhang, C. Quaternary Uranium Mineralization in the Qaidam Basin, Northern Tibetan Plateau: Insights from Petrographic and C-O Isotopic Evidences. *Ore Geol. Rev.* **2022**, *140*, 104628. [[CrossRef](#)]
86. Yan, Y.; Hu, X.; Lin, G.; Santosh, M.; Chan, L.-S. Sedimentary Provenance of the Hengyang and Mayang Basins, SE China, and Implications for the Mesozoic Topographic Change in South China Craton: Evidence from Detrital Zircon Geochronology. *J. Asian Earth Sci.* **2011**, *41*, 494–503. [[CrossRef](#)]
87. Liu, S.; Deng, B.; Zhong, Y. Unique Geologic Features of Burial and Superimposition of the Lower Paleozoic Shale Gas across the Sichuan Basin and Its Periphery. *Earth Sci. Front.* **2016**, *1*, 11–28.
88. Yang, M.; Li, L.; Zhou, J.; Qu, X.; Zhou, D. Segmentation and Inversion of the Hangjinqi Fault Zone, the Northern Ordos Basin (North China). *J. Asian Earth Sci.* **2013**, *70–71*, 64–78. [[CrossRef](#)]
89. Jin, R.; Yu, R.-A.; Yang, J.; Zhou, X.; Teng, X.; Wang, S.; Si, Q.; Zhu, Q.; Zhang, T. Paleo-Environmental Constraints on Uranium Mineralization in the Ordos Basin: Evidence from the Color Zoning of U-Bearing Rock Series. *Ore Geol. Rev.* **2019**, *104*, 175–189. [[CrossRef](#)]
90. Mei, Y.; Ren, S.; Zhang, P.; Ma, Y.; Ma, Y.; Fu, Y. Research on High-precision Gravity Scratch Analysis and Structure Features of Yili Basin, North-west China. *Geol. J.* **2019**, *54*, 1081–1089. [[CrossRef](#)]
91. Alexeiev, D.V.; Ryazantsev, A.V.; Kröner, A.; Tretyakov, A.A.; Xia, X.; Liu, D.Y. Geochemical Data and Zircon Ages for Rocks in a High-Pressure Belt of Chu-Yili Mountains, Southern Kazakhstan: Implications for the Earliest Stages of Accretion in Kazakhstan and the Tianshan. *J. Asian Earth Sci.* **2011**, *42*, 805–820. [[CrossRef](#)]
92. Jiang, S.; Li, S.; Somerville, I.D.; Lei, J.; Yang, H. Carboniferous–Permian Tectonic Evolution and Sedimentation of the Turpan-Hami Basin, NW China: Implications for the Closure of the Paleo-Asian Ocean. *J. Asian Earth Sci.* **2015**, *113*, 644–655. [[CrossRef](#)]
93. Zhu, W.; Ma, R.; Guo, J.; Sun, Y.; Guo, L.; Xu, M.; Hu, D. The Coupling of Sedimentary Characteristics and Tectonic Development of Turpan-Hami Basin and Adjacent Areas in Early Permian. *Geol. J. China Univ.* **2002**, *8*, 160–168.
94. Sun, T.; Wang, L.; Zhang, L.; Yang, H.; Zhang, Y. The Controlling Effect of Chair-Shaped Slope Break Landforms on Sedimentation in Continental Faulted Basins: A Case Study in the Xilinhalai Area, Baiyinchagan Depression, Erlian Basin, China. *Interpretation* **2022**, *10*, T567–T580. [[CrossRef](#)]
95. Zou, C.; Zhao, W.; Jia, C.; Zhu, R.; Zhang, G.; Zhao, X.; Yuan, X. Formation and Distribution of Volcanic Hydrocarbon Reservoirs in Sedimentary Basins of China. *Pet. Explor. Dev.* **2008**, *35*, 257–271. [[CrossRef](#)]
96. Wang, P.-J.; Mattern, F.; Didenko, N.A.; Zhu, D.-F.; Singer, B.; Sun, X.-M. Tectonics and Cycle System of the Cretaceous Songliao Basin: An Inverted Active Continental Margin Basin. *Earth Sci. Rev.* **2016**, *159*, 82–102. [[CrossRef](#)]
97. Li, Y.; Lu, J.; Liu, X.; Wang, J.; Ma, W.; He, X.; Mou, F.; Li, X. Geochemistry and Origins of Natural Gas in the Hong-Che Fault Zone of the Junggar Basin, NW China. *J. Pet. Sci. Eng.* **2022**, *214*, 110501. [[CrossRef](#)]
98. Bian, W.; Hornung, J.; Liu, Z.; Wang, P.; Hinderer, M. Sedimentary and Palaeoenvironmental Evolution of the Junggar Basin, Xinjiang, Northwest China. *Paleobiodivers Paleoenviron* **2010**, *90*, 175–186. [[CrossRef](#)]
99. Teng, C.; Cai, Z.; Hao, F.; Cao, Z. Structural Geometry and Evolution of an Intracratonic Strike-Slip Fault Zone: A Case Study from the North SB5 Fault Zone in the Tarim Basin, China. *J. Struct. Geol.* **2020**, *140*, 104159. [[CrossRef](#)]
100. Shuichang, Z.; Baomin, Z.; Benliang, L.; Guangyou, Z.; Jin, S.; Xiaomei, W. History of Hydrocarbon Accumulations Spanning Important Tectonic Phases in Marine Sedimentary Basins of China: Taking the Tarim Basin as an Example. *Pet. Explor. Dev.* **2011**, *38*, 1–15. [[CrossRef](#)]
101. Fu, B.; Lin, A.; Kano, K.; Maruyama, T.; Guo, J. Quaternary Folding of the Eastern Tian Shan, Northwest China. *Tectonophysics* **2003**, *369*, 79–101. [[CrossRef](#)]
102. Yin, T.; Li, S. Application of Sulfur Isotopes for Analysing the Sedimentary Environment of Evaporite in Low-Altitude Intermountain Basins: A Case Study on the Kumishi Basin, Northwest China. *Carbonates Evaporites* **2022**, *37*, 11. [[CrossRef](#)]
103. He, W.; Barzgar, E.; Feng, W.; Huang, L. Reservoirs Patterns and Key Controlling Factors of the Lenghu Oil & Gas Field in the Qaidam Basin, Northwestern China. *J. Earth Sci.* **2021**, *32*, 1011–1021. [[CrossRef](#)]
104. Hu, S.; Cao, Y.; Huang, J.; Mou, Z. Discussion on Formation and Evolution of Jurassic Basin-Prototype for Qaidam Basin. *Exp. Pet. Geol.* **1999**, *21*, 189–195.
105. Chen, P. *Paleoenvironmental Changes during the Cretaceous in Eastern China*; Elsevier: Amsterdam, The Netherlands, 2000; Volume 17, pp. 81–90.

106. Sun, S.; Li, J.; Chen, H.; Peng, H.; Kenneth, J.H.; Shelton, J. Mesozoic and Cenozoic Sedimentary History of South China. *Am. Assoc. Pet. Geol. Bull.* **1989**, *73*, 1247–1269. [[CrossRef](#)]
107. Jiao, F.; Yang, Y.; Ran, Q.; Wu, G.; Liang, H. Distribution and Gas Exploration of the Strike–Slip Faults in the Central Sichuan Basin. *Nat. Gas Ind. B* **2022**, *9*, 63–72. [[CrossRef](#)]
108. Lu, G.; Chen, X.; Zou, H.; Preto, N.; Huang, X.; Wang, C.; Shi, Z.; Jin, X. Provenance of the First Terrigenous Sediments in the Western Sichuan Basin during the Late Triassic: Implications for Basin Evolution from Marine to Continental. *Mar. Pet. Geol.* **2023**, *147*, 105992. [[CrossRef](#)]
109. Jin, R.; Liu, H.; Li, X. Theoretical System of Sandstone-Type Uranium Deposits in Northern China. *J. Earth Sci.* **2022**, *33*, 257–277. [[CrossRef](#)]
110. Jiao, Y.; Wu, L.; Rong, H.; Zhang, F. Review of Basin Uranium Resources in China. *Earth Sci.-J. China Univ. Geosci.* **2021**, *46*, 2675. [[CrossRef](#)]
111. Min, M.-Z.; Luo, X.-Z.; Du, G.-S.; He, B.-A.; Campbell, A.R. Mineralogical and Geochemical Constraints on the Genesis of the Granite-Hosted Huangao Uranium Deposit, SE China. *Ore Geol. Rev.* **1999**, *14*, 105–127. [[CrossRef](#)]
112. Min, M.; Fang, C.; Fayek, M. Petrography and Genetic History of Coffinite and Uraninite from the Liueyiqi Granite-Hosted Uranium Deposit, SE China. *Ore Geol. Rev.* **2005**, *26*, 187–197. [[CrossRef](#)]
113. Hankins, D.E. Effect of Reactivity Addition Rate and of Weak Neutron Source on the Fission Yield of Uranium Solutions. *Nucl. Sci. Eng.* **1966**, *26*, 110–116. [[CrossRef](#)]
114. Tran, E.L.; Teutsch, N.; Klein-BenDavid, O.; Weisbrod, N. Uranium and Cesium Sorption to Bentonite Colloids under Carbonate-Rich Environments: Implications for Radionuclide Transport. *Sci. Total Environ.* **2018**, *643*, 260–269. [[CrossRef](#)]
115. Jaireth, S.; McKay, A.; Lambert, I. Association of Large Sandstone Uranium Deposits with Hydrocarbons. *AusGeo News* **2009**, *89*, 1–6.
116. Spirakis, C.S. The Roles of Organic Matter in the Formation of Uranium Deposits in Sedimentary Rocks. *Ore Geol. Rev.* **1996**, *11*, 53–69. [[CrossRef](#)]
117. Liu, W.; Zhao, X.; Shi, Q.; Zhang, Z. Research on Relationship of Oil-Gas and Sandstone-Type Uranium Mineralization of Northern China. *Geol. China* **2017**, *44*, 279–287.
118. Cunningham, C.G.; Rasmussen, J.D.; Steven, T.A.; Rye, R.O.; Rowley, P.D.; Romberger, S.B.; Selverstone, J. Hydrothermal Uranium Deposits Containing Molybdenum and Fluorite in the Marysvale Volcanic Field, West-Central Utah. *Min. Depos.* **1998**, *33*, 477–494. [[CrossRef](#)]
119. Wilde, A.R.; Mernagh, T.P.; Bloom, M.S.; Hoffmann, C.F. Fluid Inclusion Evidence on the Origin of Some Australian Unconformity-Related Uranium Deposits. *Econ. Geol.* **1989**, *84*, 1627–1642. [[CrossRef](#)]
120. Ding, B.; Liu, H.; Zhang, C.; Liu, H.; Li, P.; Zhang, B. Mineralogy, Fluid Inclusion and H-O-C-S Stable Isotopes of Mengqiguer Uranium Deposit in the Southern Yili Basin, Xinjiang: Implication for Ore Formation. *Acta Geol. Sin.-Engl. Ed.* **2020**, *94*, 1488–1503. [[CrossRef](#)]
121. Heinrich, C.A. The Physical and Chemical Evolution of Low-Salinity Magmatic Fluids at the Porphyry to Epithermal Transition: A Thermodynamic Study. *Min. Depos.* **2005**, *39*, 864–889. [[CrossRef](#)]
122. Szabó, Z.; Moll, H.; Grenthe, I. Structure and Dynamics in the Complex Ion $(\text{UO}_2)_2(\text{CO}_3)(\text{OH})_3^-$. *J. Chem. Soc. Dalton Trans.* **2000**, 3158–3161. [[CrossRef](#)]
123. Bernhard, G.; Geipel, G.; Reich, T.; Brendler, V.; Amayri, S.; Nitsche, H. Uranyl(VI) Carbonate Complex Formation: Validation of the $\text{Ca}_2\text{UO}_2(\text{CO}_3)_3(\text{aq})$ Species. *Radiochim. Acta* **2001**, *89*, 511–518. [[CrossRef](#)]
124. Yue, S.; Wang, G. Relationship between the Hydrogeochemical Environment and Sandstone-Type Uranium Mineralization in the Ili Basin, China. *Appl. Geochem.* **2011**, *26*, 133–139. [[CrossRef](#)]
125. Pei, S.; Zhao, J.; Sun, Y.; Xu, Z.; Wang, S.; Liu, H.; Rowe, C.A.; Toksöz, M.N.; Gao, X. Upper Mantle Seismic Velocities and Anisotropy in China Determined through Pn and Sn Tomography. *J. Geophys. Res.* **2007**, *112*, B05312. [[CrossRef](#)]
126. Wilson, M.R.; Åkerblom, G.V. Geological Setting and Geochemistry of Uranium-Rich Granites in the Proterozoic of Sweden. *Mineral. Mag.* **1982**, *46*, 233–245. [[CrossRef](#)]
127. Guthrie, V.A.; Kleeman, J.D. Changing Uranium Distributions during Weathering of Granite. *Chem. Geol.* **1986**, *54*, 113–126. [[CrossRef](#)]
128. Skierszkan, E.K.; Dockrey, J.W.; Mayer, K.U.; Beckie, R.D. Release of Geogenic Uranium and Arsenic Results in Water-Quality Impacts in a Subarctic Permafrost Region of Granitic and Metamorphic Geology. *J. Geochem. Explor.* **2020**, *217*, 106607. [[CrossRef](#)]
129. Parsons, I.; Lee, M.R.; Smith, J.V. Biochemical Evolution II: Origin of Life in Tubular Microstructures on Weathered Feldspar Surfaces. *Proc. Natl. Acad. Sci. USA* **1998**, *95*, 15173–15176. [[CrossRef](#)] [[PubMed](#)]
130. Zhou, Q.; Liu, S.; Xu, L.; Zhang, H.; Xiao, D.; Deng, J.; Pan, Z. Estimation of Radon Release Rate for an Underground Uranium Mine Ventilation Shaft in China and Radon Distribution Characteristics. *J. Environ. Radioact.* **2019**, *198*, 18–26. [[CrossRef](#)]
131. Ma, K.; Cui, L.; Dong, Y.; Wang, T.; Da, C.; Hirasaki, G.J.; Biswal, S.L. Adsorption of Cationic and Anionic Surfactants on Natural and Synthetic Carbonate Materials. *J. Colloid Interface Sci.* **2013**, *408*, 164–172. [[CrossRef](#)] [[PubMed](#)]
132. Guo, T. Key Controls on Accumulation and High Production of Large Non-Marine Gas Fields in Northern Sichuan Basin. *Pet. Explor. Dev.* **2013**, *40*, 150–160. [[CrossRef](#)]

133. Toens, P.D.; Andrews-Speed, C.P. The Time-Bound Character of Uranium Mineralising Processes, with Special Reference to the Proterozoic of Gondwana. *Precambrian Res.* **1984**, *25*, 13–36. [[CrossRef](#)]
134. Adams, S.; Smith, R. *Geology and Recognition Criteria for Sandstone Uranium Deposits in Mixed Fluvial-Shallow Marine Sedimentary Sequences, South Texas. Final Report*; OSTI.GOV: Oak Ridge, TN, USA, 1981.

Disclaimer/Publisher’s Note: The statements, opinions and data contained in all publications are solely those of the individual author(s) and contributor(s) and not of MDPI and/or the editor(s). MDPI and/or the editor(s) disclaim responsibility for any injury to people or property resulting from any ideas, methods, instructions or products referred to in the content.